Effect of Interchain Interaction on Optical Properties of Poly(*p*-phenylene vinylene) Derivative Containing Oxadiazole in Backbone

Fan Kong,[1] Wendan Fang,[1] Yimin Yang,[2] Teng Qiu[2]

[1]*School of Chemistry and Chemical Engineering, Southeast University, Nanjing 211189, People's Republic of China*
[2]*Department of Physics, Southeast University, Nanjing 211189, People's Republic of China*

Received 4 November 2010; accepted 20 February 2011
DOI 10.1002/app.34383
Published online 24 June 2011 in Wiley Online Library (wileyonlinelibrary.com).

ABSTRACT: We have investigated the optical properties of poly [2-methoxy-5-(2-ethylhexyloxy)-1,4-phenylene vinylene] containing oxadiazole in backbone (MEH-OPPV) in dilute tetrahydrofuran solution and solid solution films. There is a large dihedral angle between the two adjacent monomer units in MEH-OPPV, which restrains interchain interactions and destroys the conjugation of the polymer to result in blue shifted absorption and emission spectra. The red shifted photoluminescence (PL) peak is continuously changed in the solid solution films with increasing the concentration of MEH-OPPV. Comparison with the dilute solution, an obvious shoulder peak at 465 nm is found in the UV–vis absorption and PL excitation (PLE) spectra of the MEH-OPPV film. The intensity of the PLE shoulder at 465 nm is increased with the concentration of MEH-OPPV in the solid solution films, which is connected with the aggregation of the MEH-OPPV chains. The interchain interactions are restrained and the π-stack aggregates of the polymer chains can not form in the MEH-OPPV due to the large dihedral angle, and then the interchain species are effectively suppressed in the MEH-OPPV films. © 2011 Wiley Periodicals, Inc. J Appl Polym Sci 122: 2583–2587, 2011

Key words: conjugated polymers; photophysics; interchain interactions; fluorescence

INTRODUCTION

Conjugated polymers have attracted increasing interest because of their potential application in optoelectronics, such as light-emitting diodes (LEDs), solid lasers, solar cells, and biosensors.[1–4] Poly (*p*-phenylene vinylene) and its derivatives (PPVs) are one family of most promising polymers for application in optoelectronic devices. The conjugated polymer chains consist of many segments with different conjugation lengths, contributing to broad emission spectra and large Stocks shifts due to excitation energy transfer from short segments to low energy sites. The interchain interactions play an essential role on the photophysics of the conjugated polymers in films or nanostructures. The energy transfer in the conjugated polymers can be achieved along backbone or through interchain interactions.[5] The former type energy transfer depends on the chain structures. Dihedral angle will be increased if the two adjacent monomer units have markedly different symmetries and orbital energies.[6] Large dihedral angle is usually unfavorable of the intrachain energy transfer and increases the distance of the polymer chains, which observably impresses the interchain energy transfer.[7]

Controlling the interchain interactions is an important way to optimize the performances of the optoelectronic devices based on the conjugated polymers.[5] Comparison with the solution, the red shifted emissions are often observed in the conjugated polymer films, which have been attributed to various causations including extended polymer chains,[8] strong polarization interaction of the excited state with the environment,[9] or the interchain species.[10,11] There are multiple interchain excited states, such as spacial indirect excitons,[12,13] excimers[14,15] or aggregates,[9,10,16] going with the interchain interactions. The interchain species depend on the supramolecular effect of chemical structure and chain arrangement.[15–17] The emissions from intrachain excitons or interchain species can be adjusted by adding other molecules or polymers to improve the performance of optoelectronic devices.[18,19] Thus, it is very important to adjust

Correspondence to: F. Kong (kongfan@seu.edu.cn).
Contract grant sponsor: National Natural Science Foundation of China under; contract grant number: 51071045.
Contract grant sponsor: Specialized Research Fund for the Doctoral Program of Higher Education; contract grant number: 200802861065.
Contract grant sponsor: Technology Fund of Southeast University; contract grant number: KJ20100431.

the interchain interactions for controlling the excitation energy transfer, the carrier transport and the interchain species in the conjugated polymers.

The equilibriums of the injections and the transports of carriers are necessary to obtain high performance polymer LEDs. Aryl oxadiazole with large electron affinity introduced into the conjugated polymers can effectively balance carrier transports. In this work, we investigated the optical properties of poly [2-methoxy-5-(2-ethylhexyloxy)-1,4-phenylene vinylene] containing oxadiazole in backbone (MEH-OPPV) in tetrahydrofuran (THF), film, and an inert polymer, polystyrene (PS). The experimental results show that there is no obvious interchain species formed in MEH-OPPV. By analyzing the photoluminescence (PL) and PL excitation (PLE) spectra of MEH-OPPV in the dilute solution, film and the solid solution films, the emission from the MEH-OPPV film originates from intrachain excitons. The interchain interactions broaden the average electron bands of MEH-OPPV to result in low energy gaps. So the continuously red shifted PL peaks have been observed in the PL spectra of the solid solution films with increasing the concentration of MEH-OPPV. Hence, controlling the interchain interaction is a facile way to modify the electrical and optical properties of the conjugated polymer films.

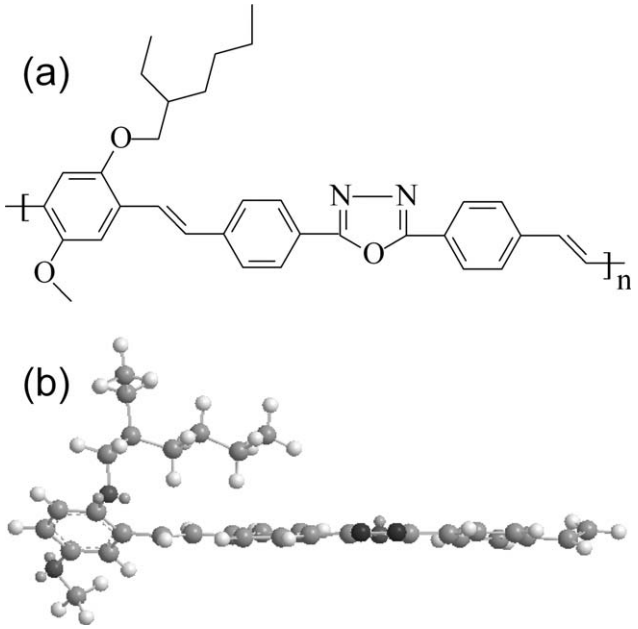

Figure 1 (a) Chemical structure of MEH-OPPV, (b) Stereo depiction of the lowest energy conformation of MEH-OPPV.

EXPERIMENTAL

MEH-OPPV was synthesized via a Wittig condensation reaction, which has been described in our previous literature.[20] The chemical structure of MEH-OPPV is shown in Figure 1(a). The inert polymer PS (from Acros Organics) was used as received without any purification. MEH-OPPV and PS were dissolved in THF to form the solutions with the concentration of 2 mg/mL, respectively. And then the two kinds of the polymer solutions were blended with different proportions. The weight ratios of MEH-OPPV to PS in the blend THF solutions were 1/1000, 1/100, 1/50, 1/20, 1/10, 1/5, 1/1, and 1/0, respectively. The solid solution films of MEH-OPPV/PS were prepared by spin-coating the blended THF solutions on clean glass substrates. The concentration of the MEH-OPPV solution is diluted to be 0.1 mg/mL for measuring UV–vis absorption and emission spectra. The polymer films were spin-coated on patterned indium tin oxide (ITO) substrates, and then aluminum was evaporated onto the polymer films to form sandwich structured devices (ITO/polymer/Al). Current-voltage characteristics of the devices were measured on an Agilent 4156C precision semiconductor parameter analyzer. The PL and PLE spectra of the polymer films or the electroluminescence (EL) spectra of the devices were obtained using the Fluorolog-3 fluorescence spectrophotometer (HORIBA Jobin Yvon). The absorption spectra of the samples were acquired by a Shimadzu UV-3100 spectrophotometer. All the experiments were performed at room temperature.

RESULTS AND DISCUSSION

Figure 1(b) shows the stereo depiction of the lowest energy conformations of MEH-OPPV, generated by employing a conformational research using MM2 force field as implemented in ChemDraw Ultra 7.0. There is an approximately 35° dihedral angle between the two adjacent monomer units in the MEH-OPPV due to the conjugation between the nitrogen lone pair electrons and the π-electrons.[21] The π-electron delocalization along the MEH-OPPV chain is restricted by the nonplanar conformation caused by rotation along the C—C bond. As a result, the PL spectrum of MEH-OPPV is markedly blue shifted relative to MEH-PPV with a planar conformation.

Figure 2 shows the optical properties of MEH-OPPV in the dilute THF solution. The PL peak of the dilute MEH-OPPV solution is blue shifted to 487 nm, while the PL peak of the MEH-PPV solution is usually at 550 nm. There are two peaks at 320 nm and 370 nm in the absorption spectrum of the dilute MEH-OPPV solution. Similar absorption band with peak at 320 nm has been found in other conjugated polymers containing heterocyclic rings in backbone or side chain.[21–23] Heterocyclic rings are introduced into conjugated polymers to increase the relative intensity of the 320-nm absorption band due to sole

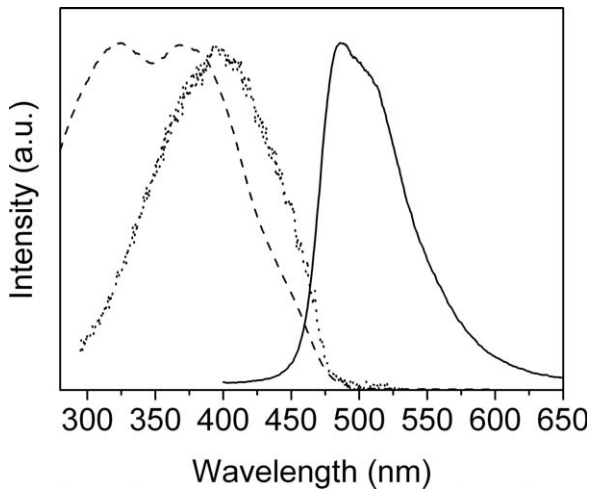

Figure 2 UV–vis absorption (dashed line), PL (solid line, excitation at 380 nm), and PLE (dotted line, monitored at the emission wavelength of 550 nm) spectra of the MEH-OPPV solution with the concentration of 0.1 mg/mL.

pair electrons. So, the absorption peak at 320 nm is corresponding to $n \rightarrow \pi^*$ transitions. The $n \rightarrow \pi^*$ electron transition originates from the sole pair electrons (*n*-electrons) in N and O atoms in oxadiazole groups, whereas the $\pi \rightarrow \pi^*$ electron transition is from the π-electrons in aromatic vinyl structures. Compared with the UV–vis absorption spectrum, only one peak at 395 nm is observed in the PLE spectrum and the peak at 320 nm is disappeared. This implies that the *n*-electron transition is invalid for the PL of the dilute MEH-OPPV solution. So, the emission from MEH-OPPV in the dilute solution originates from π-electron transition, which is in practical use for polymer optoelectronic devices.

Usually, the PL spectra of the conjugated polymer in the films are red shifted relative to those in the solutions due to the interchain interactions. Figure 3 shows the UV–vis absorption, PL and PLE spectra of the MEH-OPPV film. It can be seen that the PL peak of the MEH-OPPV film is red shifted to 520 nm. Similar to the solution, the UV–vis absorption spectrum of the MEH-OPPV film has two peaks, corresponding to $n \rightarrow \pi^*$ and $\pi \rightarrow \pi^*$ electron transitions, respectively. There is an obvious shoulder at 465 nm in the UV–vis absorption spectrum, which becomes distinct in the PLE spectrum of the MEH-OPPV film. The polymer chains are separated by the solvent in the dilute solution, whereas the polymer chains are aggregated in the film. The energy bands are broadened to reduce the band gap of the polymer in the film due to the interchain interactions. The aggregated polymer chains with low energy gaps contribute to the red shifted absorption and emission spectra of the polymer film. Thus, the 465-nm absorption band is connected with the ground states with low excitation energies in the MEH-OPPV film, contributing to the red shifted PL spectrum.

For investigating the effect of the interchain interactions on the emission from MEH-OPPV, we have measured the PL spectra of the MEH-OPPV solid solution films, as shown in Figure 4. No emission from PS is observed as the pure PS film is photoexcited at 360 nm. There is an accessional and weird PL shoulder at 420 nm in the PL spectra of the dilute solid solution films, which does not appear in the PL spectrum of the dilute THF solution. Comparison with aryl oxadiazole, it can be inferred that the PL shoulder originates from the excited states in the isolated aryl oxadiazole groups.[23] The intensity

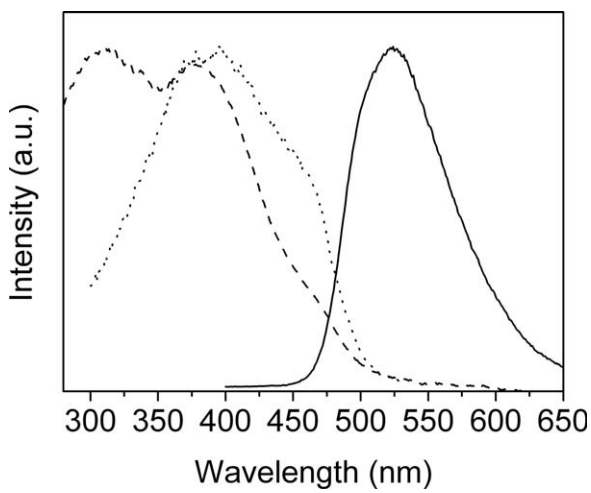

Figure 3 UV–vis absorption (dashed line), PL (solid line, excitation at 380 nm), and PLE (dotted line, monitored at the emission wavelength of 550 nm) spectra of the MEH-OPPV film.

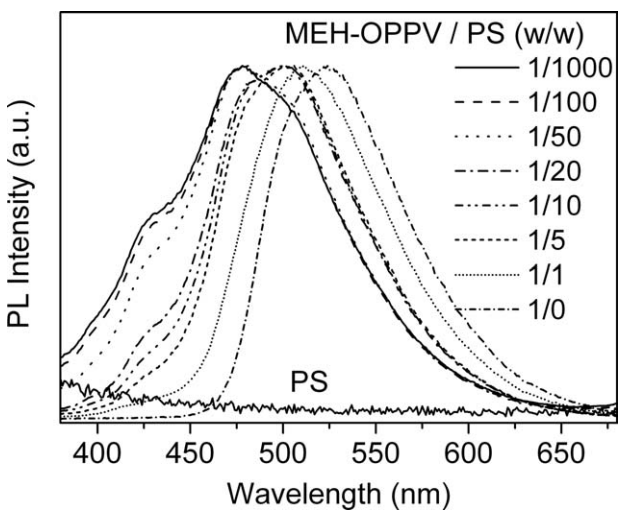

Figure 4 Normalized PL spectra of the solid solution films of MEH-OPPV/PS (excitation at 360 nm). The weight ratios of MEH-OPPV to PS are 1/1000, 1/100, 1/50, 1/20, 1/10, 1/5, 1/1, and 1/0, respectively.

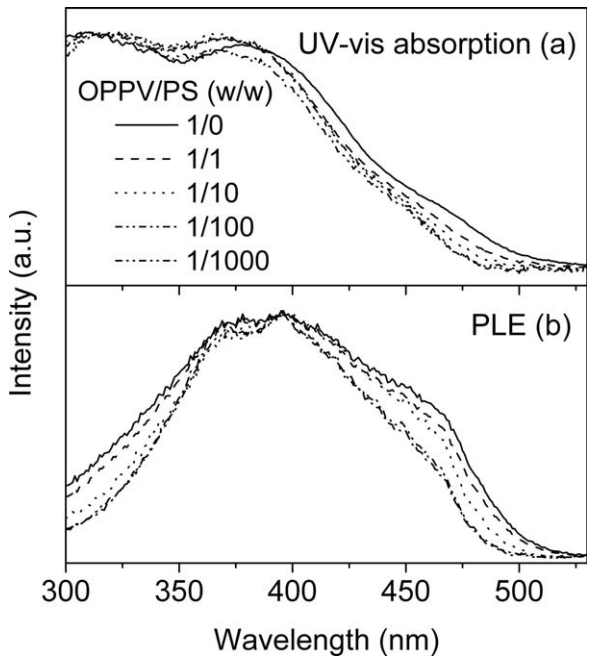

Figure 5 Normalized UV–vis absorption and PLE spectra of the solid solution films of MEH-OPPV/PS measured under the monitoring emission wavelength of 550 nm. The weight ratios of MEH-OPPV to PS are 1/1000, 1/100, 1/10, 1/1, and 1/0, respectively.

of the PL shoulder at 420 nm is decreased with increasing the concentration of MEH-OPPV and disappears in the pure MEH-OPPV film. It has been proved that the exciton migration along the polymer backbone is much slower than through interchain interactions, especially for large dihedral angles in the polymer chains.[5,7] The large dihedral angle in the backbone limits π-electron delocalization and exciton migration in a single polymer chain of MEH-OPPV. As a result, the PL shoulder at 420 nm is observed in the dilute MEH-OPPV solid solution films since the MEH-OPPV chains are separated by PS to eliminate the interchain energy transfer. Normally, the interchain interaction is in favor of resonance energy transfer from high energy sites to low energy sites. As the concentration of MEH-OPPV is increased in the solid solution films, more excited states in the aryl oxadiazole groups with high energies are transferred to long conjugation segments through the interchain interactions. So the PL intensity at 420 nm is decreased in the solid solution films with high concentrations of MEH-OPPV, and until disappears in the MEH-OPPV film.

It can be seen from Figure 4 that the PL peaks are red shifted from 480 nm to 520 nm with increasing the concentration of MEH-OPPV in the solid solution films. Different from MEH-PPV,[10] the PL peak wavelength changes are continuous in the PL spectra of the MEH-OPPV solid solution films. All the monomer units are nearly coplanar in MEH-PPV, in which the polymer chains favorably form the aggregates due to π-stack.[24] There are two kinds of monomer unites in MEH-OPPV, which are named as phenylene vinylene and aryl-substituted oxadiazole. The differences in symmetries and orbital energies of the two adjacent monomer units destroy the planar conformation of the copolymer, resulting in the large dihedral angle between the two adjacent monomer units in the MEH-OPPV. The large dihedral angle restrains the interchain interaction and makes the MEH-OPPV chains to form the aggregated states with π-stacks difficultly. Thus, there is no distinct emission from the aggregates or other interchain species observed in MEH-OPPV. It is reasonable to be considered that the red shifted emission from the MEH-OPPV film originates from the radiative recombination of the intrachain excitons with low energy gaps due to the weak interchain interactions.

The UV–vis absorption spectra of the MEH-OPPV solid solution films are described in Figure 5(a). It can be seen that the absorption edges are red-shifted with increasing the MEH-OPPV concentration. The results infer that the optical band gap of the conjugated polymer is decreased with the concentration of MEH-OPPV due to the increased interchain interaction. The effect of the interchain interactions on the optical properties of MEH-OPPV can be further investigated by PLE spectra. Figure 5(b) shows the PLE spectra of MEH-OPPV in the solid solution films measured under the monitoring emission wavelength of 550 nm. It can be seen that the PLE bands of the solid solution films become broad with increasing the MEH-OPPV concentration. The intensity of the PLE shoulder at 465 nm is increased with the concentration of MEH-OPPV due to the increasing interchain interactions.

As discussed above, the luminescence quantum yield of the MEH-OPPV film should be higher than that of the MEH-PPV film since there is a lack of the interchain excited states in the MEH-OPPV film. The luminescence quantum yield of the copolymer MEH-OPPV film (η_{co}) relative to that of the homopolymer MEH-PPV film (η_{ho}) can be calculated by the following equation[25]:

$$\frac{\eta_{co}}{\eta_{ho}} = \frac{A_{ho}(\lambda_{exc})}{A_{co}(\lambda_{exc})}\frac{D_{co}}{D_{ho}}\frac{n_{co}^2}{n_{ho}^2} \quad (1)$$

where A_{co} and A_{ho} are the absorbances of the MEH-OPPV film and the MEH-PPV film. n_{co} and n_{ho} are their refractive indices, and D_{co} and D_{ho} are the integrated emission intensities over the entire PL spectra of the MEH-OPPV film and the MEH-PPV film, respectively. The luminescence quantum yield of the MEH-OPPV film is 1.46 times of that of the MEH-PPV film. The result indicates that the interchain

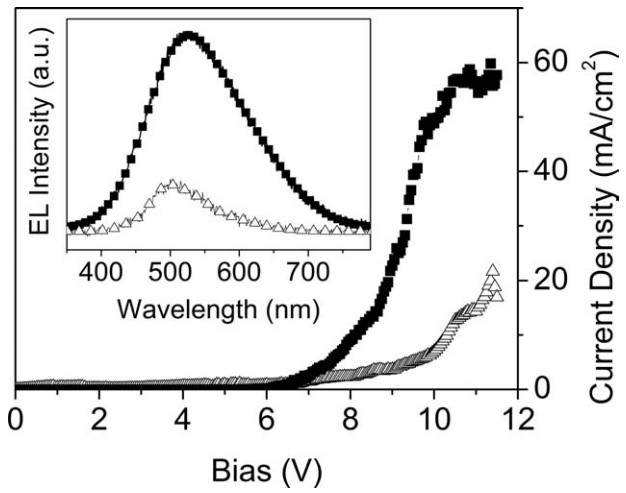

Figure 6 Current density-voltage characteristics of the devices of ITO/MEH-OPPV/Al (■) and ITO/MEH-OPPV : PS(1/1, w/w)/Al (Δ), with the inset showing the EL spectra of the devices.

excited states with low luminescence quantum yields are suppressed in the MEH-OPPV film. The interchain interactions in MEH-OPPV are decreased by the nonplanar conformation of the polymer backbone. The weak interchain interactions limit the interchain species with low luminescence efficiencies formed in the copolymer film. So the fluorescence quantum efficiency of the conjugated copolymer film is usually higher than that of the conjugated homopolymer film due to less exciton quenching in the copolymer.[22,23]

The inert polymer introduced into the active layer of the polymer LED can decrease its conductivity because the electron transition barrier is increased. We measured the electrical properties of the polymer LEDs with or without PS in the active layers. Figure 6 shows the current density–voltage characteristics of the devices. It can be clearly seen that the inert polymer adding into the active layer increase the turn-on voltage of the polymer LEDs due to the low conductivity of the active layer containing PS. The inset in Figure 6 describes the EL spectra of the devices, which are obtained under 9 V for ITO/MEH-OPPV/Al and 10 V for ITO/MEH-OPPV : PS/Al, respectively. The EL peaks of the devices nearly correspond to the PL peaks of their active layers, but the EL spectrum of the device without PS becomes wider than the PL spectrum of the MEH-OPPV film, which often caused by Joule thermal effect at high current.[26,27]

CONCLUSIONS

We have presented the optical properties of MEH-OPPV in the THF solution, film and solid solution films. The large dihedral angle between the two adjacent monomer units destroys the conjugation of the polymer, contributing to the blue shifted absorption and emission spectra. The PL peak of the MEH-OPPV solid solution film is red shifted continuously with increasing the concentration of MEH-OPPV. The interchain interactions are restrained and the π-stack structures for interchain species can not form in the MEH-OPPV due to the large dihedral angle, and then the interchain species with low luminescence efficiencies, such as aggregates or excimers, are effectively suppressed in the MEH-OPPV films.

References

1. Friend, R. H.; Gymer, R. W.; Holmes A. B.; Burroughes, J. H.; Marks, R. N.; Taliani, C.; Bradley, D. D. C.; Santos, D. A. D.; Bredas, J. L.; Logdlund, M.; Salaneck, W. R. Nature 1999, 397, 121.
2. McGehee, M. D.; Heeger, A. J. Adv Mater 2000, 12, 1655.
3. McQuade, D. T.; Pullen, A. E.; Swager, T. M. Chem Rev 2000, 100, 2537.
4. McNeill, C. R.; Greenham, N. C. Adv Mater 2009, 21, 3840.
5. Nguyen, T. Q.; Wu, J. J.; Doan, V.; Schwartz, B. J.; Tolbert, S. H. Science 2000, 286, 652.
6. Chen, L. X.; Jalger, W. J. H.; Niemczyk, M. P.; Wasielewski, M. R. J Phys Chem A 1999, 103, 4341.
7. Yang, J. S.; Yan, J. L.; Lin, C. K.; Chen, C. Y.; Xie, Z. Y.; Chen, C. H. Angew Chem Int Ed 2009, 48, 9936.
8. Shi, Y.; Liu, J.; Yang, Y. J Appl Phys 2000, 87, 4254.
9. Nguyen, T. Q.; Martini, I. B.; Liu, J.; Schwartz, B. J. J Phys Chem B 2000, 104, 237.
10. Kong, F.; Wu, X. L.; Yuan, R. K.; Yang, C. Z.; Siu, G. G.; Chu, P. K. J Vac Sci Technol A 2006, 24, 202.
11. Samuel, I. D. W.; Rumbles, G.; Collison, C. J.; Friend, R. H.; Moratti, S. C.; Holmes, A. B. Synth Met 1997, 84, 497.
12. Yan, M.; Rothberg, L. J.; Papadimitrakopoulos, F.; Galvin, M. E.; Miller, T. M. Phys Rev Lett 1994, 72, 1104.
13. Yan, M.; Rothberg, L. J.; Kwock, E. W.; Miller, T. M. Phys Rev Lett 1992 1995, 75.
14. Samuel, I. D. W.; Rumbles, G.; Collison, C. J Phys Rev B 1995, 52, 11573.
15. Wu, M. W.; Conwell, E. M. Phys Rev B 1997, 56, 10060.
16. Peng, K. Y.; Chen, S. A.; Fann, W. S.; Chen, S. H.; Su, A. C. J Phys Chem B 2005, 109, 9368.
17. Traiphol, R.; Charoenthai, N.; Srikhirin, T.; Kerdeharoen, T.; Osotchan, T.; Maturos, T. Polymer 2007, 48, 813.
18. Marletta, A.; Goncalves, V. C. Balogh, D. T. J Lumin 2006, 116, 87.
19. Krautz, D.; Lunedei, E.; Puigdollers, J.; Badenes, G.; Alcubilla, R.; Cheylan, S. Appl Phys Lett 2010, 96, 033301.
20. Zhang, S. Y. Kong, F.; Sun, R.; Yuan, R. K.; Jiang, X. Q.; Yang, C. Z. J Appl Polym Sci 2003, 89, 2618.
21. Tsai, F. C.; Chang, C. C.; Liu, C. L.; Chen, W. C. Jenekhe, S. A. Macromolecules 1958, 2005, 38.
22. Jin, S. H.; Kim, M. Y.; Kim, J. Y.; Lee, K.; Gal, Y. S. J Am Chem Soc 2004, 126, 2474.
23. Su, W. F.; Yeh, K. M.; Chen, Y. J. Polym Sci Part A: Polym Chem 2007, 45, 4377.
24. Kong, F.; Wu, X. L.; Huang, G. S.; Yuan, R. K.; Yang, C. Z.; Chu, P. K.; Siu, G. G. Appl Phys A 2006, 84, 203.
25. Chou, H. L.; Lin, K. F.; Fan, Y. L.; Wang, D. C. J Polym Sci Part B: Polym Phys 2005, 43, 1705.
26. Braun, D.; Moses, D.; Zhang, C.; Heeger, A. J Appl Phys Lett 1992, 61, 3092.
27. Ding, L.; Lu, Z.; Egbe, D. A. M.; Karasz, F. E. Macromolecules 2004, 37, 10031.